

No-Reference Quality Assessment for Colored Point Cloud and Mesh Based on Natural Scene Statistics

Zicheng Zhang(✉), Wei Sun, Xionguo Min, Tao Wang, Wei Lu, and Guangtao Zhai
Institute of Image Communication and Network Engineering, Shanghai Jiao Tong University, China
zzc1998@sjtu.edu.cn

Abstract—To improve the viewer’s quality of experience and optimize processing systems in computer graphics applications, the 3D quality assessment (3D-QA) has become an important task in the multimedia area. Point cloud and mesh are the two most widely used electronic representation formats of 3D models, the quality of which is quite sensitive to operations like simplification and compression. Therefore, many studies concerning point cloud quality assessment (PCQA) and mesh quality assessment (MQA) have been carried out to measure the visual quality degradations caused by lossy operations. However, a large part of previous studies utilizes full-reference (FR) metrics, which means they may fail to predict the accurate quality level of 3D models when the reference 3D model is not available. Furthermore, limited numbers of 3D-QA metrics are carried out to take color features into consideration, which significantly restricts the effectiveness and scope of application. In many quality assessment studies, natural scene statistics (NSS) have shown a good ability to quantify the distortion of natural scenes to statistical parameters. Therefore, we propose an NSS-based no-reference quality assessment metric for colored 3D models. In this paper, quality-aware features are extracted from the aspects of color and geometry directly from the 3D models. Then the statistic parameters are estimated using different distribution models to describe the characteristic of the 3D models. Our method is mainly validated on the colored point cloud quality assessment database (SJTU-PCQA) and the colored mesh quality assessment database (CMDM). The experimental results show that the proposed method outperforms all the state-of-art NR 3D-QA metrics and obtains an acceptable gap with the state-of-art FR 3D-QA metrics.

Index Terms—3D-QA, Colored point cloud, Colored mesh, No-reference, PCQA, MQA, NSS

I. INTRODUCTION

A. Motivation

Nowadays, with the rapid development of computer graphics, the digital representation of 3D models has been widely studied and used in a wide range of application scenarios such as virtual reality (VR), medical 3D reconstruction, and video post-production [1]. Among the common digital representation forms of 3D models, point cloud and mesh are the most widely used formats in practical. A point cloud is a set of data points in space, in which each point is described with geometry coordinates and sometimes with other attributes such as color and surface normals. Mesh is more complicated because it is a collection of vertices, edges, and faces which together define the shape of a 3D model. Additionally, except for geometry information, the 3D mesh may also contain various

appearance attributes, such as color and material. Both point cloud and mesh are able to vividly display exquisite models and complex scenes, however, they may take up relatively large storage space at the same time. Limited by unstable application environment and fixed transmission bandwidth especially on mobile light-weighted devices, diverse 3D algorithms are proposed to adapt to specific needs using processing operations such as simplification and compression, which inevitably cause damage to the visual quality of 3D models. Additionally, in some scanning 3D model APIs like Apple 3D object capture [2] and Intel Lidar Camera Realsense [3], some slight disturbance like blur and noise may be introduced to the constructed 3D models, especially when color information is included as well.

Therefore, to improve viewer’s Quality of Experience (QoE) in 3D fields and optimize 3D compression and reconstruction systems, it is of great significance to develop metrics for point cloud quality assessment (PCQA) and mesh quality assessment (MQA). However, different from the format of 2D media like image and video where pixels are distributed in the fixed grid, the 3D model’s points are distributed irregularly in the space, which brings a huge challenge for 3D quality assessment tasks. The neighborhood for pixels in 2D media can be easily obtained, thus the local features are available by analyzing the relationship between the pixel and its neighborhood. However, the neighborhood for points in 3D models is very ambiguous, which makes it difficult to construct local feature analysis. Furthermore, the shape for 2D media is fixed, which enables us to easily scale or crop the 2D media for feature extraction while similar operations are hard to define for 3D models. Although many 3D-QA databases [4] [5] [6] [7] have been proposed to push forward the development of 3D-QA algorithms, the difficulty of collecting 3D models and conducting subjective experiments greatly limit the size of the 3D-QA databases, which may also restrict relevant research, especially for NR 3D-QA metrics.

B. Previous 3D-QA works

It is known that subjective quality assessment is time-consuming and expensive, thus objective quality metrics are urgently needed to predict the quality level of 3D models automatically. The objective quality assessment can then be divided into FR 3D-QA methods and NR 3D-QA methods. Considering the complexity of 3D models, in the literature, a large part of proposed metrics only take geometry features into

consideration [8] [9] [10] [11]. When it comes to 3D models with color information, limited numbers of works have been proposed [12] [13] [14]. In this section, we briefly review the development of 3D-QA and explicitly list some of the mainstream methods designed for 3D-QA tasks.

1) *The development of PCQA*: Many mainstream PCQA metrics only operate on the geometry aspect at the point level, such as p2point [8], p2plane [9], and p2mesh [15]. The p2point estimates the levels of distortion by computing the distance vector between the corresponding points. The p2plane further projects the distance vector on the normal orientation for evaluating the quality loss. The p2mesh first reconstructs the point cloud to mesh and then measures the distance from point to the reconstructed surface to predict the quality level, which greatly depends on the reconstruction algorithms and lacks stability. Metrics based on more complicated geometry features are then proposed. Alexiou *et al.* [16] adopt the angular difference of point normals to estimate the degradations. Javaheri *et al.* [17] utilize the generalized Hausdorff distance to reflect the distortions caused by compression operations.

The metrics mentioned above are all FR-PCQA metrics that only focus on geometry information. However, in some situations, color information can not be ignored. Therefore, Meynet *et al.* use the weighted linear combination of curvature and color information to evaluate the visual quality of distorted point cloud. Inspired by SSIM [18], Alexiou *et al.* [19] employ the SSIM formulation to compute the similarity on four types of features, including geometry, normal vectors, curvature and color information. What's more, some studies [4] [7] try to predict the quality level by evaluating the projected 2D images from 3D models. The advantage is that 2D image quality assessment (IQA) metrics have been well developed and the disadvantage is quite obvious: there is inevitable information loss during the projected operation.

There are few NR-PCQA metrics developed due to the lack of large-scale PCQA database. Recently, a large-scale PCQA database with 24,752 distorted point clouds has been constructed [20] and the author proposes a learning-based approach for NR-PCQA. However, the database has not been publicly available yet.

2) *The development of MQA*: Supported by the vast amount of previous research on 2D-QA tasks [21] [22] [23] [24] [25], many objective metrics have been introduced to deal with MQA problems using similar ideas, which usually function by computing local features at the vertex level and then pooling the features into a quality value. MSDM2 [10] used the differences of structure (captured via curvature statistics) computed on local corresponding neighborhoods from the meshes being compared to predict the quality level. DAME [26] measure the differences in dihedral angles between the reference and the distorted meshes to evaluate the quality loss. FMPD [11] estimates the local roughness difference derived from Gaussian curvature to assess the quality of distorted mesh. All these metrics mentioned only take geometry information into consideration and are full-reference. To analyze the influence of color information, Tian *et al.* [12] introduces a global distance over texture image using Mean Squared Error (MSE) to quantify the effect of color information. And Guo *et*

al. [13] exploit SSIM to calculate the texture image distance as the color information features.

Recently, thanks to the effectiveness of machine learning, many MQA metrics based on machine learning have been proposed. Abouelaziz *et al.* [27] extract features using dihedral angle models and train a support vector machine for feature regression. Later, Abouelaziz *et al.* [28] scale the curvature and dihedral angle into 2D patches and utilize convolution neural network (CNN) for training. Again, Abouelaziz *et al.* [29] further introduces a CNN framework with saliency views rendered from 3D meshes.

In summary, the MQA metrics can be categorized into two types: model-based metrics [10] [26] [11] [27] [28] which operate directly on the 3D models and image quality assessment (IQA) metrics [12] [13] [29] [30] [31] which operate on the rendering snapshots of 3D models. The IQA metrics can effectively extract the quality features from the snapshots with the mature development of IQA methods. However, affected by diverse viewpoints and complicated animations, the IQA metrics may not be stable and precise when predicting the quality of 3D meshes. Therefore, model-based metrics are more suitable and effective for MQA meshes since the mesh model is invariant to the viewpoints.

C. Our approach

Generally speaking, a large part of the metrics mentioned are full-reference, which can make full use of the relationship between the reference and distorted 3D models and gives relatively accurate results. But FR 3D-QA metrics' disadvantage is also obvious, they are not able to function in the absence of reference models. And in many application scenarios like 3D reconstruction, pristine reference is not always available. Therefore, inspired by the huge success of NSS in 2D-QA tasks [32] [21], we further expand NSS to 3D-QA tasks. NSS is a discipline within the field of perception, which is dependent on the premise that the perceptual system is designed to interpret natural scenes [33]. NSS-based methods operate by estimating the statistic parameters of feature distributions to quantify the distortion of natural scenes, which indicates that such methods are not sensitive to the shape and distribution pattern of data.

To address the problem of no-reference quality assessment for both colored point cloud and mesh, we propose a novel metric to predict the visual quality levels of 3D models based on natural scene statistics (NSS). In particular, we first project the 3D models into different feature domains, which include color and geometry aspects. Then we utilize different distribution models to estimate statistic parameters of different feature domains. For point cloud, the geometry features include curvature, anisotropy, linearity, planarity, and sphericity. For mesh, the geometry features consist of curvature, dihedral angle, face area, and face angle. For both point cloud and mesh, the color is converted from RGB color space to LAB color space for feature extraction. Inspired by NSS QA metrics, mean, variance, the generalized Gaussian distribution parameters, the general asymmetric generalized Gaussian distribution parameters, and the shape-rate Gamma distribution

parameters are employed to capture the characteristics of each feature domain's distribution. Finally, the statistic parameters are integrated into a quality value through the support vector regression (SVR) model. In order to test the effectiveness of different types of features and different kinds of distribution models, we also test the performance of different combinations of the statistic parameters. The experimental result shows that our method outperforms the mainstream NR metrics for 3D model quality assessment and obtains an acceptable gap with the state-of-art FR 3D-QA metrics.

D. Contributions

We summarize our contributions as follows:

- To the best of our knowledge, we first introduce the NSS concept, which has been widely adopted in many 2D quality assessment (2D-QA) studies, to 3D-QA fields.
- We conduct a no-reference quality assessment metric for both colored point cloud and mesh. The features are extracted from the color and geometry aspects. For point cloud, the geometry features include curvature, anisotropy, linearity, planarity, and sphericity. For mesh, the geometry features consist of curvature, dihedral angle, face area, and face angle. What's more, the feature extraction and regression framework are very standard, which means it is easy to modify our metric for specific needs and performance improvement.
- We further discuss the effectiveness of different types of features (color and geometry) and different kinds of distribution models. The performance results are clearly shown in the experiment section.

The paper is organized as follows: Section II describes the feature projection processes. Section III describes the NSS models used to quantify the distortions to statistical parameters. Section IV presents the experiment set up along with the experimental results. Section V summaries the content of this paper and gives some ideas on further exploration.

II. FEATURE PROJECTION

In order to explain our method more explicitly, we define the given distorted point cloud and distorted mesh:

$$P = \{Points\}, \quad (1)$$

$$M = \{Vertices, Edges, Faces\}, \quad (2)$$

where the color information is attached to *Points* in the point cloud and *Vertices* in mesh respectively.

A. Geometry Feature Projection

Geometry features usually have a strong correlation with human perception that has been firmly proved in 3D-QA studies. Although the geometry features are computed in different ways for point cloud and mesh, they share similar quality characteristics for the visual quality of 3D models. Thus in this section, we project the given 3D models into several quality-aware geometry feature domains:

$$F_{geo} = Projection_{geo}(P, M), \quad (3)$$

where F_{geo} indicates the set of geometry feature domains of the 3D model, $Projection_{geo}(\cdot)$ denotes for the geometry projection function, and P and M represent the distorted point cloud and mesh respectively.

B. Point Cloud Geometry Feature Domains

Considering that the point cloud lacks surfaces, some necessary approaches have to be adopted to lay the foundation for the extraction of geometry features. Given the point cloud $P = \{p_i\}_{i=1}^N$, the neighborhood N_i of each vertex p_i can be obtained utilizing the k-nearest neighbors (k-NN) algorithm:

$$N = KNN_{k=10}(P), \quad (4)$$

$$Dist(p, q) = \sqrt{(p_x - q_x)^2 + (p_y - q_y)^2 + (p_z - q_z)^2}, \quad (5)$$

where N is the neighborhood set of N_i , $KNN(\cdot)$ denotes the k-NN algorithm function, the k level is set as 10, and Euclidean distance is exploited as the distance function. With the neighborhood, the corresponding covariance matrix C for each point p_i can be computed as:

$$C = \begin{bmatrix} p_1 - \bar{p} \\ \vdots \\ p_{K_0} - \bar{p} \end{bmatrix}^T \cdot \begin{bmatrix} p_1 - \bar{p} \\ \vdots \\ p_{K_0} - \bar{p} \end{bmatrix}, p_{i=1, \dots, K_0} \in N_i \quad (6)$$

where K_0 stands for the size of neighborhood N_i , and \bar{p} represents the centroid of neighbors in N_i . Therefore, the eigenvector problem for the covariance matrix C can be described as below:

$$C \cdot v_j = \lambda_j \cdot v_j, j \in \{1, 2, 3\} \quad (7)$$

where $(\lambda_1, \lambda_2, \lambda_3)$ indicate the eigenvalues, (v_1, v_2, v_3) represent the corresponding eigenvectors, and we assume that $\lambda_1 > \lambda_2 > \lambda_3$. Thus, a total of 3 eigenvalues are obtained for each point p_i in the point cloud P .

In previous studies [34] [35], the eigenvalues mentioned above are used to calculate various geometry features for tasks like classification, simplification, and segmentation. And the computed features show great ability to describe the complicated geometry information and achieve outstanding performance in the above tasks. Hence, we selected several geometry features that may be effective for point cloud quality assessment as follows:

- **Curvature:** Curvature is the amount by which a curve deviates from being a straight line, which is frequently used to describe roughness or smoothness.
- **Anisotropy:** Anisotropy is used to exhibit variations in geometrical properties for different directions.
- **Linearity:** Linearity is the property for estimating the similarity to a straight line.
- **Planarity:** Planarity is utilized to measure the similarity to planar surface.
- **Sphericity:** Sphericity is the measure of how closely the shape of an object resembles that of a perfect sphere.

Additionally, all the geometry features described above are calculated at the point level, which indicates that each p_i has its

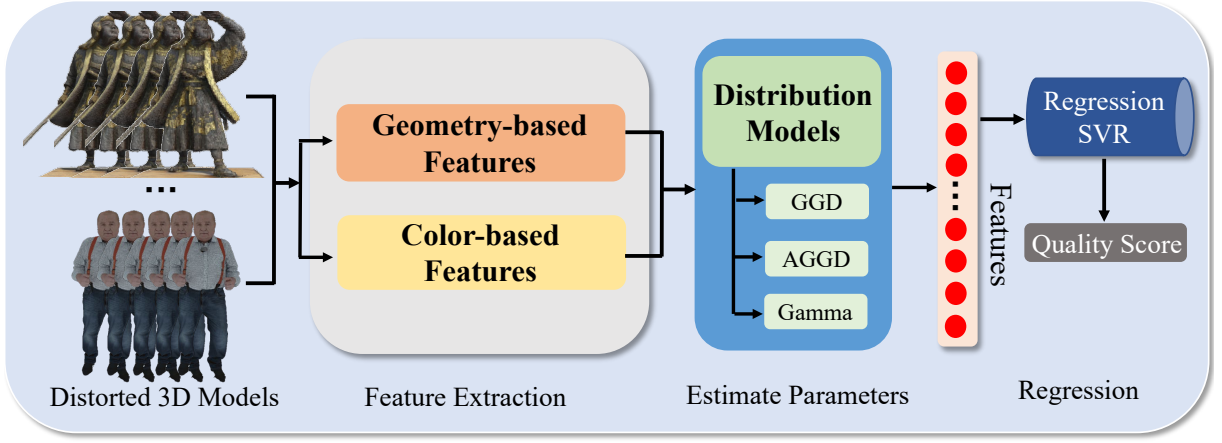


Fig. 1. Framework of the proposed method.

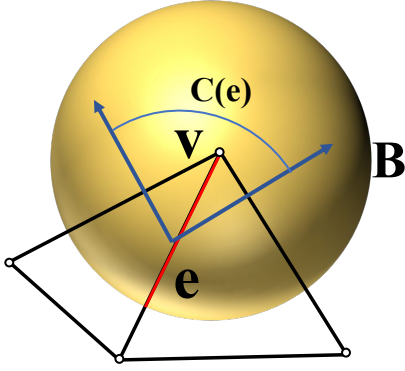


Fig. 2. Example of the variables corresponding to the curvature calculation, where the red line indicates $|e \cap B|$ and $C(e)$ indicates the curvature contribution of e .

own curvature, anisotropy, linearity, planarity, and sphericity. The formulations for geometry features are denoted as:

$$Cur(p_i) = \frac{\lambda_3}{\lambda_1 + \lambda_2 + \lambda_3}, \quad (8)$$

$$Ani(p_i) = \frac{\lambda_1 - \lambda_3}{\lambda_1}, \quad (9)$$

$$Lin(p_i) = \frac{\lambda_1 - \lambda_2}{\lambda_1}, \quad (10)$$

$$Pla(p_i) = \frac{\lambda_2 - \lambda_3}{\lambda_1}, \quad (11)$$

$$Sph(p_i) = \frac{\lambda_3}{\lambda_1}, \quad (12)$$

where λ_1, λ_2 , and λ_3 refer to the corresponding eigenvalues respectively. Through the operations mentioned above, the point cloud is transformed to 5 geometry feature domains.

C. Mesh Geometry Feature Domains

Among the common digital representation forms of 3D models, the 3D mesh is more complicated because it is a collection of vertices, edges, and faces which together define the shape of a 3D model. Therefore, the feature extraction is different from that in the point cloud.

1) *Curvature*: Curvature has always been a critical attribute in numerous studies concerning 3D quality assessment issues due to its strong correlation with representative visual characteristics like roughness or smoothness. Thanks to the edges and faces information contained in mesh, the computation of curvature is more precise than the point cloud. So far, various curvature definitions have been introduced for 3D meshes [36] [37], among which the average curvature is proven to be able to stably describe the local structural information of 3D meshes. Hence, a weighted average curvature method introduced in [37] is adopted to measure the roughness of embedded surfaces in 3D meshes. Given the mesh $M = \{v_i\}_{i=1}^N$, the weighted average curvature is calculated by averaging the curvature contributions over a certain region B around each vertex:

$$Cur(v_i) = \frac{1}{|B|} \sum_{e \in E} C(e) |e \cap B| \cdot \bar{e} \bar{e}^t, \quad (13)$$

where $Cur(v_i)$ represents the weighted average curvature for vertex v , region B is a sphere region centered at v and its radius is $1/100$ of the bounding box of the 3D mesh, $|B|$ stands for the surface area of region B . E is the set of edges that are linked to the vertex v , $C(e)$ indicates the curvature contribution of e (the signed angle between the normals of the two oriented triangles incident to edge e), $|e \cap B|$ denotes the weight which is defined as the length of $e \cap B$ (always between 0 and $|e|$) and \bar{e} is a unit vector in the same direction as e . An example of the variables corresponding to the curvature calculation is shown in Fig. 2.

2) *Dihedral Angle*: Normally speaking, dihedral angle is the angle between two planes. For a 3D mesh, the dihedral angle is the angle between the normals of two adjacent faces, which has been utilized in [38] as an effective indicator for measuring the loss of the mesh simplification. Furthermore, [26] exploits oriented dihedral angles instead of the simple dot product of normals to better distinguish the convex and concave angles, which achieves great performance. Encouraged by similar ideas, we adopt the dihedral angles set to describe the visual quality of 3D meshes. Assuming that the vertices for two adjacent faces f_1 and f_2 are $\{v_1, v_3, v_4\}$ and

$\{v2, v3, v4\}$, we have:

$$Dih_{f_1, f_2} = \arccos(n_1 \cdot n_2) * \text{sgn}(n_1 \cdot (v_2 - v_1)), \quad (14)$$

where D_{f_1, f_2} is the oriented dihedral angle between two adjacent faces f_1 and f_2 , n_1 and n_2 are the normals of f_1 and f_2 , sgn denotes the signum function which is used to decide the orientation of the dihedral angle.

3) *Face Area and Angle*: Area and angle are two simple attributes of 3D mesh faces, which can be easily computed by making use of the coordinates of the face's vertices. In the mesh smoothing algorithm proposed in [39], attributes including face angle are used to predict the new location of the smoothed nodes. While in the 3D mesh encoding method introduced in [40], face angle is utilized to instruct the compression of 3D meshes, which indicates that face angle is related to the quality of 3D meshes. Therefore, to further measure the visual quality degradation of 3D meshes, the face area and angle are collected as feature sets.

Finally, the mesh is projected into 4 geometry feature domains:

- *Curvature*: The weighted average curvature is used to describe the geometry characteristics like roughness or smoothness.
- *Dihedral Angle*: Dihedral angle is employed as a useful descriptor for measuring the caused degradations.
- *Face Area & Angle*: These two attributes are highly correlated with the effectiveness of lossy operations like compression.

D. Color Feature Projection

Color is a significant aspect of visual quality assessment. The color information in the 3D models is usually stored in the form of RGB channels, which has been proven to have a poor correlation with human perception. Additionally, the color presentation is different between point cloud and mesh. For a colored point cloud, the color is directly determined by the color information of the point, while for a colored mesh, the color of the surface is generally rendered by the color information of the contained vertices.

We can see clearly from Fig. 4 that with the increase of color distortion level, the visual quality is damaged more severely. Since the color distortion is generated by quantization in the CMDM database, the corresponding probability distributions become more separated when the color distortion level rises. To better analyze the influence of color information, we convert the color information from RGB channels to LAB channels, which has been adopted in many quality assessment tasks [5] as the color projection for 3D models:

$$F_{color} = \text{Projection}_{color}(P, M), \quad (15)$$

where F_{color} indicates the set of color feature domains of the 3D model, $\text{Projection}_{color}(\cdot)$ stands for the color projection function, and P and M represent the distorted point cloud and mesh respectively. And the detailed color transformation is formulated as below:

$$\begin{bmatrix} X \\ Y \\ Z \end{bmatrix} = \begin{bmatrix} 2.7688 & 1.7517 & 1.1301 \\ 1.0000 & 4.5906 & 0.0601 \\ 0 & 0.0565 & 5.5942 \end{bmatrix} \begin{bmatrix} R \\ G \\ B \end{bmatrix}, \quad (16)$$

$$\begin{cases} L &= 116f\left(\frac{Y}{Y_n}\right) - 16, \\ A &= 500\left(f\left(\frac{X}{X_n}\right) - f\left(\frac{Y}{Y_n}\right)\right), \\ B &= 200\left(f\left(\frac{Y}{Y_n}\right) - f\left(\frac{Z}{Z_n}\right)\right), \end{cases} \quad (17)$$

where R, G, B represent the corresponding RGB color channels, X, Y, Z stand for the corresponding XYZ color channels, L, A, B denote the corresponding RGB color channels, and X_n, Y_n, Z_n describe a specified white achromatic reference illuminant. The $f(\cdot)$ function is described as:

$$f(t) = \begin{cases} \sqrt[3]{t}, & \text{if } t > \delta^3, \\ \frac{t}{3\delta^2} + \frac{4}{29}, & \text{otherwise,} \end{cases} \quad (18)$$

where δ is set as $\frac{6}{29}$. Therefore, the LAB color channels are computed as the color feature domains.

III. ESTIMATE NSS PARAMETERS

In this section, we plan to discuss the process of estimating NSS parameters. Through prior knowledge and observations of the corresponding feature distributions, we select several NSS models to fit the feature distributions. To determine the effectiveness of different NSS models, we perform several experiments for validation. To be specific, the geometry and color information is computed at the point level for the colored point cloud. However, for the colored mesh, the curvature and color information is computed at the vertex level, the dihedral angle is calculated at the edge level, while the face area and angle are computed at the face level.

A. Basic Statistical Parameters

With the set of various features, we exploit the normalization operation as the pre-processing:

$$\hat{F} = \frac{F - \text{mean}(F)}{\text{std}(F) + C}, \quad (19)$$

$$F \in \{F_{geo}, F_{color}\}, \quad (20)$$

where F represents the feature domain, $\text{mean}(\cdot)$ is the average function, $\text{std}(\cdot)$ denotes the standard deviation function, and F_{geo} and F_{color} indicate the geometry and color feature domains respectively. The average and standard deviation values of each feature domain are collected as the first set of statistical parameters. Fig. 4 presents the LAB normalized distributions of the color quantization distortion. It can be observed that with the increasing quantization levels, the corresponding distributions become significantly sparse. Considering that some simplification and compression algorithms usually introduce such quantization operations to the 3D models, hence, we propose to use entropy to measure the information loss:

$$E = \text{entropy}(F), \quad (21)$$

$$F \in \{F_{geo}, F_{color}\}, \quad (22)$$

B. GGD Parameters

It can be observed from Fig. II-D that the feature distributions tend to be Gaussian-like, especially for the geometry distributions after distorted operations. And clearly with the

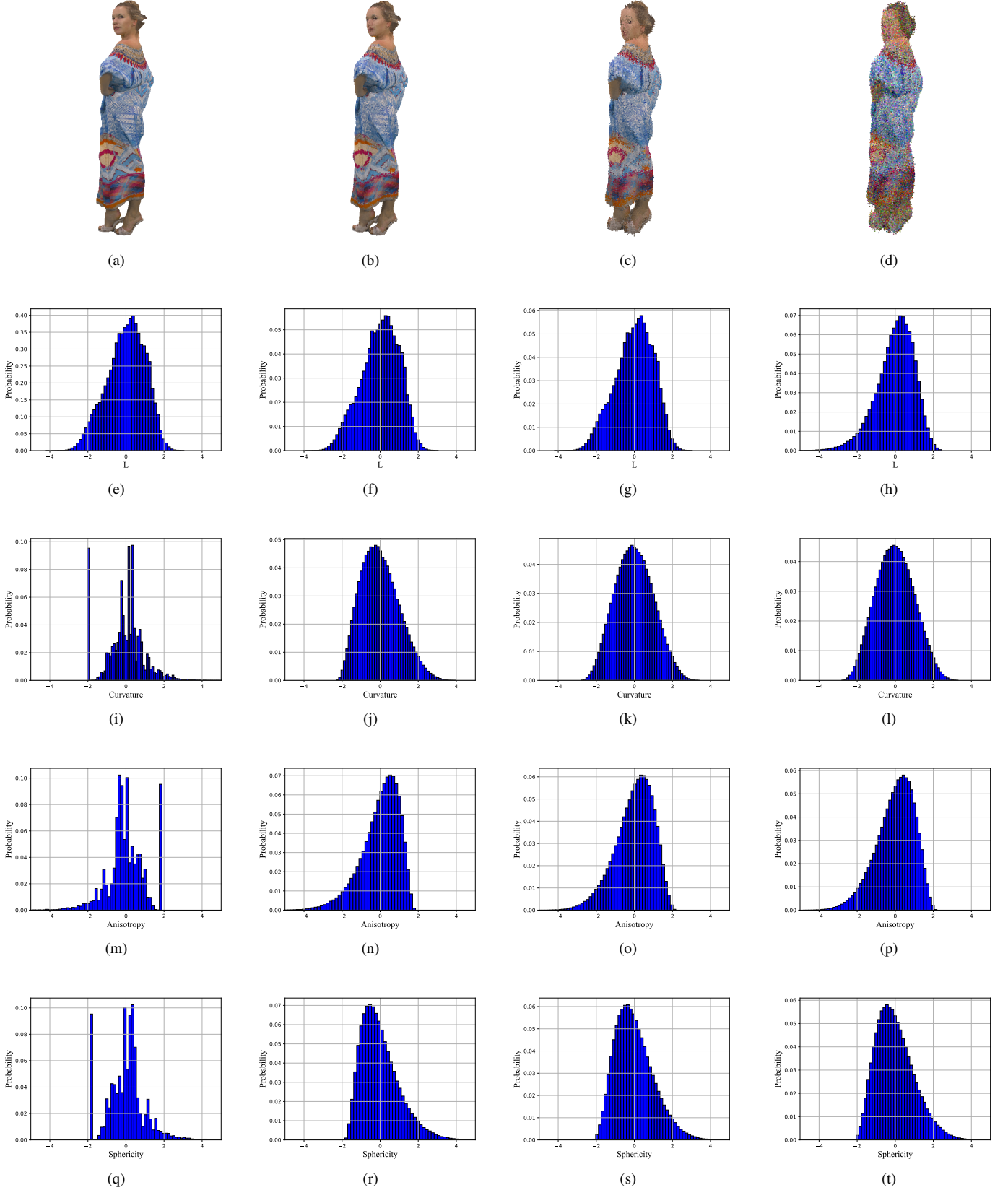


Fig. 3. Examples of point cloud samples from SJTU-PCQA database [4]. (a), (b), (c), and (d) are 4 distorted point cloud samples with increasing distortion level. Some features' normalized probability distributions are selected to as examples. More specifically, (e), (i), (m), and (q) are the corresponding (L, Cur, Ani, Sph) features' normalized probability distributions of (a) model, (f), (j), (n), and (r) are the corresponding (L, Cur, Ani, Sph) features' normalized probability distributions of (b) model, (g), (k), (o), and (s) are the corresponding (L, Cur, Ani, Sph) features' normalized probability distributions of (c) model, (h), (l), (p), and (t) are the corresponding (L, Cur, Ani, Sph) features' normalized probability distributions of (d) model respectively.

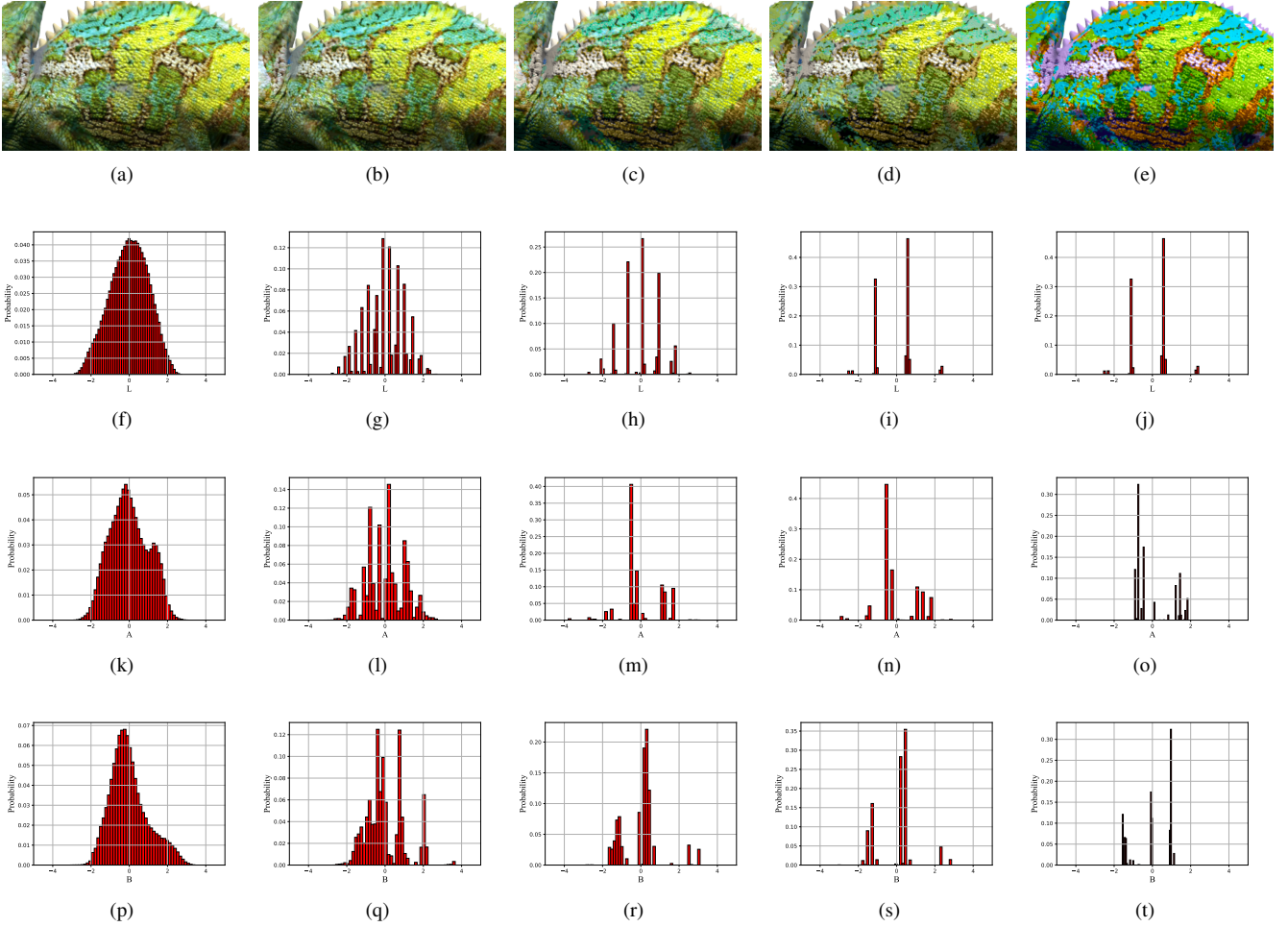


Fig. 4. A comparison example for color distortion in the CMDM database [5]. (a) represents the snapshots of the reference 3D mesh while (b)-(e) stands for the snapshots of the meshes with 4 increasing levels of color information quantization. (f), (k), (p) represent the LAB probability distributions for (a), (g), (l), (q) represent the LAB probability distributions for (b), (h), (m), (r) represent the LAB probability distributions for (c), (i), (n), (s) represent the LAB probability distributions for (d), and (j), (o), (t) represented the LAB probability distributions for (e) respectively.

higher level of distortions, the shape and scale of the distributions vary from each other. To capture the characteristics of 3D model distributions at the general level, we propose to use the generalized Gaussian distribution (GGD) :

$$GGD(x; \alpha, \beta^2) = \frac{\alpha}{2\beta\Gamma(1/\alpha)} \exp\left(-\left(\frac{|x|}{\beta}\right)^\alpha\right), \quad (23)$$

$$x \in \{F_{geo}, F_{color}\},$$

where $\beta = \sigma \sqrt{\frac{\Gamma(1/\alpha)}{\Gamma(3/\alpha)}}$, $\Gamma(\alpha) = \int_0^\infty t^{\alpha-1} e^{-t} dt$, $\alpha > 0$ is the gamma function, and the two estimated parameters (α, β^2) indicate the shape and variance of the distribution. What's more, considering that the variance for normalized distribution is fixed as 1, we estimate the GGD parameters from distributions before normalization.

C. AGGD Parameters

However, in some situations, the shape of the distribution is not symmetrical. We can see clearly from Fig. II-D that the anisotropy distributions for the (b)-(d) models have longer

tails on the left while the sphericity distributions for the (b)-(d) models have longer tails on the right. Inspired by [21], we utilize the general asymmetric generalized Gaussian distribution (AGGD) model to extract more detailed parameters from normalized feature distributions to describe the different spread extent in two directions:

$$AGGD(x; v, \sigma_l^2, \sigma_r^2) = \begin{cases} \frac{v}{(\beta_l + \beta_r)\Gamma(\frac{1}{v})} \exp\left(-\left(\frac{-x}{\beta_l}\right)^v\right) & x < 0, \\ \frac{v}{(\beta_l + \beta_r)\Gamma(\frac{1}{v})} \exp\left(-\left(\frac{x}{\beta_r}\right)^v\right) & x \geq 0, \end{cases}$$

$$x \in \{F_{geo}, F_{color}\}, \quad (24)$$

where $\beta_l = \sigma_l \sqrt{\frac{\Gamma(\frac{1}{v})}{\Gamma(\frac{3}{v})}}$, $\beta_r = \sigma_r \sqrt{\frac{\Gamma(\frac{1}{v})}{\Gamma(\frac{3}{v})}}$, $\eta = (\beta_r - \beta_l)$, the parameter v decides the shape of the distribution, σ_l^2 and σ_r^2 are scale parameters that refer to the spread extent on the left and right side of the distribution respectively, η is a parameter that can better fit the AGGD model stated in [21]. Additionally, the AGGD can be recognized as the extension of GGD. Furthermore, when $\sigma_l^2 = \sigma_r^2$, the AGGD turns into GGD. The four parameters $(\eta, v, \sigma_l^2, \sigma_r^2)$ are able to obtain more representative characteristics of asymmetric distribution.

D. Gamma parameters

In many 3D-QA studies [41], Gamma distribution is usually employed as the estimated distribution and has been proven effective. Hence, we also adopt Gamma distribution to estimate statistical parameters. The shape-rate Gamma model is formulated as:

$$\text{Gamma}(x; \alpha, \beta) = \frac{\beta^\alpha x^{\alpha-1} e^{-\beta x}}{\Gamma(\alpha)} x > 0, \quad (25)$$

$$x \in \{\hat{F}_{geo}, \hat{F}_{color}\},$$

where α and β stands for the shape and rate parameters and $\alpha, \beta > 0$.

In summary, we collect the average, standard deviation, and entropy values as the fundamental features. Then we use 3 representative distribution models to estimate 8 statistical parameters, including GGD (α, β^2), AGGD ($\eta, v, \sigma_l^2, \sigma_t^2$), Gamma (α, β), for all feature domains. Finally, considering that the colored point cloud has 8 feature domains ($Cur, Ani, Lin, Pla, Sph, L, A, B$) and the colored mesh has 7 feature domains ($Cur, Dhi, Far, Fan, L, A, B$), 88 (8×11) features are computed for a single colored point cloud and 77 (7×11) features are computed for a single colored mesh respectively. The summary of features extracted in the proposed method is listed in Tab. I.

E. Regression Model

After the feature extraction process, a feature vector is obtained to describe the characteristics of the 3D model. In our experiment, we propose to use the support vector machine regressor (SVR) as the regression model, which is a common and effective choice to handle high dimensional data in previous quality assessment research [21] [27]. Then the feature vector can be integrated into a quality score for evaluation. We employ the Python sklearn package to implement the radial basis function (RBF) kernel SVR model with the default settings.

IV. EXPERIMENT EVALUATION

A. Experiment Setup

Four mainstream consistency evaluation criteria are utilized to compare the correlation between the predicted scores and MOSs, which include Spearman Rank Correlation Coefficient (SRCC), Kendall's Rank Correlation Coefficient (KRCC), Pearson Linear Correlation Coefficient (PLCC), Root Mean Squared Error (RMSE).

1) *Experiment Setup for PCQA*: To test the performance of the proposed method, we utilize the subjective point cloud assessment (SJTU-PCQA) database introduced in [4]. The SJTU-PCQA database provides 420 point cloud samples distorted from 10 reference point clouds. Each reference point cloud is distorted with seven types of common distortions, including compression noise, color noise, Gaussian geometric shift, downsampling loss, etc. And each kind of distortion is adjusted with six levels, which generates 42 (7×6) distorted point cloud samples for every reference point cloud. Unfortunately, only 9 reference point clouds and their corresponding

distorted point cloud samples are now available in the public, thus we can obtain 378 (9×42) point cloud samples for validation.

Since the proposed approach requires a training procedure to calibrate the SVR model and to avoid the point cloud samples distorted from the same reference point cloud from appearing in the training and testing procedure at the same time, we select 7 of the 9 groups of point clouds as training set and leave the rest 2 groups as testing set. In order to ensure the validity of the results, we exhaustively list all the $C_9^7=36$ database separations for the experiment and use the average performance as the final experimental result. To maintain the same experiment evaluation setup in [4], we select SRCC, PLCC, and RMSE as the judging criteria.

Considering that limited numbers of no-reference QA metrics for colored point clouds have been proposed (the learning-based no-reference approach in [20] has not open source yet), we select mostly full-reference metrics for comparison. The comparison QA metrics can be categorized into two types:

- 3D-to-2D metrics: These metrics evaluate the quality of 3D models by assessing the quality of the corresponding 2D projections. Please refer to [4] for detailed projection setup. The 2D QA metrics include PSNR, SSIM [18], MS-SSIM [22], IW-SSIM [42], FSIM [23], VIF [24], NIQE [43], and PB-PCQA[4].
- Model-based metrics: These metrics operate directly from the 3D model, which include p2point [8], p2plane [9], and PCQM [14].

Additionally, only NIQE is a no-reference metric and the rest metrics are all full-reference. To further test the effectiveness and contributions of different types of features (color and geometry) and different distribution models, we split the features into 6 groups and obtain the performance of different combinations of feature groups: (1) P1: mean, standard deviation, and entropy values of color feature domains; (2) P2: GGD parameters of color feature domains; (3) P3: GGD parameters of color feature domains; (4) Gamma distribution parameters of color feature domains; (5) P5: mean, standard deviation, and entropy values of geometry feature domains; (6) P6: GGD parameters of geometry feature domains; (7) P7: AGGD parameters of geometry feature domains; (8) P8: Gamma distribution parameters of geometry feature domains.

2) *Experiment Setup for MQA*: The method proposed in this paper is validated on the color mesh distortion measure (CMDM) database [5]. The database is generated from 5 source models subjected to geometry and color distortions. Then the source models are corrupted with 4 types of distortions based on color and geometry and each type of distortion is adjusted with 4 different strengths. The selected distortions are able to represent the common visual quality loss, which can usually be perceived during typical 3D model processing. In all, there are 80 distorted models in this database and each distorted model is provided with 5 subjective scores according to its viewpoints and animation types. For simplification, we use the average of the 5 subjective scores as the final quality score for the distorted model.

Similarly in the literature, few metrics are proposed to deal with the QA tasks of 3D color meshes. In order to evaluate the

TABLE I
SUMMARY OF FEATURES EXTRACTED IN THE PROPOSED METHOD

| Type | Feature Domains | Feature ID | NSS models | Computation |
|-------------|--------------------------------------|---------------------|---|-------------|
| Point cloud | $(Cur, Ani, Lin, Pla, Sph, L, A, B)$ | $f_{p1} - f_{p16}$ | Mean and standard deviation for each feature domain | Eq.(20) |
| | $(Cur, Ani, Lin, Pla, Sph, L, A, B)$ | $f_{p17} - f_{p24}$ | Entropy for each feature domain | Eq.(22) |
| | $(Cur, Ani, Lin, Pla, Sph, L, A, B)$ | $f_{p25} - f_{p40}$ | GGD (α, β^2) for each feature domain | Eq.(23) |
| | $(Cur, Ani, Lin, Pla, Sph, L, A, B)$ | $f_{p43} - f_{p72}$ | AGGD $(\eta, v, \sigma_l^2, \sigma_t^2)$ for each normalized feature domain | Eq.(24) |
| | $(Cur, Ani, Lin, Pla, Sph, L, A, B)$ | $f_{p73} - f_{p88}$ | Gamma (α, β) for each normalized feature domain | Eq.(25) |
| Mesh | $(Cur, Dhi, Far, Fan, L, A, B)$ | $f_{m1} - f_{m14}$ | Mean and standard deviation for each feature domain | Eq.(20) |
| | $(Cur, Dhi, Far, Fan, L, A, B)$ | $f_{m15} - f_{m21}$ | Entropy for each feature domain | Eq.(22) |
| | $(Cur, Dhi, Far, Fan, L, A, B)$ | $f_{m22} - f_{m35}$ | GGD (α, β^2) for each feature domain | Eq.(23) |
| | $(Cur, Dhi, Far, Fan, L, A, B)$ | $f_{m36} - f_{m63}$ | AGGD $(\eta, v, \sigma_l^2, \sigma_t^2)$ for each normalized feature domain | Eq.(24) |
| | $(Cur, Dhi, Far, Fan, L, A, B)$ | $f_{m64} - f_{m77}$ | Gamma (α, β) for each normalized feature domain | Eq.(25) |

TABLE II
PERFORMANCE COMPARISON WITH COMPETITORS ON THE SJTU-PCQA DATABASE.

| Type | Metric | PLCC | SRCC | RMSE |
|-------------|------------------|---------------|---------------|---------------|
| 3D-to-2D | PSNR (FR) | 0.2481 | 0.2512 | 2.3354 |
| | SSIM (FR) | 0.3654 | 0.2789 | 2.2440 |
| | MS-SSIM (FR) | 0.3659 | 0.2592 | 2.2437 |
| | IW-SSIM (FR) | 0.4339 | 0.3285 | 2.1720 |
| | FSIM (FR) | 0.3196 | 0.3019 | 2.2843 |
| | VIF (FR) | 0.5243 | 5647 | 2.0653 |
| | NIQE (NR) | 0.3262 | -0.1149 | 2.2788 |
| | PB-PCQA (FR) | 0.6076 | 0.6020 | 1.8635 |
| Model-based | p2point (FR) | 0.0466 | 0.7009 | 2.4081 |
| | p2plane (FR) | 0.0462 | 0.6881 | 2.4080 |
| | PCQM (FR) | 0.8603 | 0.8465 | 1.2291 |
| Proposed | P1+P5 (NR) | 0.7522 | 0.7449 | 1.7004 |
| | P2+P6 (NR) | 0.7173 | 0.6973 | 1.7581 |
| | P3+P7 (NR) | 0.6106 | 0.6122 | 2.0208 |
| | P4+P8 (NR) | 0.5841 | 0.4999 | 2.0469 |
| | P1+P2+P3+P4 (NR) | 0.2351 | 0.2408 | 2.4511 |
| | P5+P6+P7+P8 (NR) | 0.7314 | 0.7137 | 1.8096 |
| | All groups (NR) | 0.7294 | 0.6887 | 1.8059 |

TABLE III
PERFORMANCE COMPARISON WITH COMPETITORS ON THE CMDM DATABASE.

| Type | Metric | PLCC | SRCC | KRCC | RMSE |
|-------------|------------------|---------------|---------------|---------------|---------------|
| 3D-to-2D | PSNR (FR) | 0.7672 | 0.7735 | 0.7280 | 0.8832 |
| | SSIM (FR) | 0.7944 | 0.7817 | 0.7000 | 0.9656 |
| | MS-SSIM (FR) | 0.8112 | 0.8029 | 0.8167 | 1.0019 |
| | FSIM (FR) | 0.7786 | 0.8264 | 0.7800 | 1.0245 |
| | VIF (FR) | 0.7901 | 0.7882 | 0.7333 | 0.8800 |
| | NIQE (FR) | 0.4059 | 0.4768 | 0.3000 | 1.3352 |
| | BRISQUE (FR) | 0.5786 | 0.4882 | 0.3598 | 1.2237 |
| | NR-SVR (FR) | 0.6082 | 0.4489 | 0.3420 | 1.3147 |
| Model-based | NR-GRNN (FR) | 0.6599 | 0.6948 | 0.5130 | 1.1121 |
| | NR-CNN (FR) | 0.5204 | 0.5022 | 0.3420 | 1.2804 |
| | CMDM (FR) | 0.9130 | 0.9000 | - | - |
| Proposed | M1+M5 (NR) | 0.8781 | 0.8530 | 0.6955 | 0.6019 |
| | M2+M6 (NR) | 0.7819 | 0.7392 | 0.5821 | 0.7646 |
| | M3+M7 (NR) | 0.8342 | 0.7974 | 0.6456 | 0.6989 |
| | M4+M8 (NR) | 0.5982 | 0.5262 | 0.3951 | 0.9956 |
| | M1+M2+M3+M4 (NR) | 0.2985 | 0.1820 | 0.2283 | 1.2469 |
| | M5+M6+M7+M8 (NR) | 0.6561 | 0.5076 | 0.3954 | 0.9267 |
| | All groups (NR) | 0.8826 | 0.8754 | 0.7222 | 0.6062 |

performance of the proposed method, some quality assessment metrics that might be able to predict the visual quality of 3D meshes are utilized as competitors. Unfortunately, few no-reference quality assessment metrics for 3D meshes are open-sourced, thus we try to reproduce some of the metrics. Specifically, the metrics used for comparison can be divided into two types:

- 3D-to-2D metrics: Full-reference and No-reference image quality assessment metrics which may be effective by evaluating the quality of 2D images rendered from the 3D color meshes: PSNR [18], SSIM [22], MS-SSIM [22], IW-SSIM [42], FSIM [23], VIF [24], NIQE [43], and BRISQUE [21].
- Model-based metrics: No-reference quality assessment

metrics designed especially for 3D meshes usually without color: NR-SVR [27], NR-GRNN [44], NR-CNN [28].

For the same purpose to evaluate the effectiveness and contributions of different features, we categorize the features into 6 feature groups as well: (1) M1: mean, standard deviation, and entropy values of color feature domains; (2) M2: GGD parameters of color feature domains; (3) M3: GGD parameters of color feature domains; (4) M4: Gamma distribution parameters of color feature domains; (5) M5: mean, standard deviation, and entropy values of geometry feature domains; (6) M6: GGD parameters of geometry feature domains; (7) M7: AGGD parameters of geometry feature domains; (8) M8: Gamma distribution parameters of geometry feature domains.

B. Performance Discussion

1) *PCQA on the SJTU-PCQA Database*: The experimental results for PCQA on the SJTU-PCQA database are shown in Tab. II and the top 2 performance results in each column are marked in bold. We can see clearly that the FR-PCQA metric PCQM outperforms other PCQA metrics, which indicates that PCQM is effective at predicting the quality levels of distorted point clouds. The P1+P5 combination of our proposed method achieves second place. Although the best performance of our method still has a gap with PCQA, our method is more competitive than the widely used p2point and p2plane. And considering that our method does not need original point clouds for reference, we can draw the conclusion that the proposed method does have a certain ability to extract quality-aware features and gives relatively accurate quality levels for distorted meshes.

Further, the P1+P2+P3+P4 combination represents feature groups with only color features and the P5+P6+P7+P8 combination represents feature groups with only geometry features. It can be observed that the geometry features contribute more to the final quality score on the SJTU-PCQA database. By analyzing the different performance of different distribution models, we can see that the AGGD model achieves the poorest performance while the mean, standard deviation, and entropy values obtain the best performance, which indicates that the simpler statistic parameters can capture more representative characteristics on the SJTU-PCQA database.

2) *MQA on the CMDM Database*: Tab. III presents the experimental results on the CMDM database and the top 2 performance results in each column are marked in bold. The FR-MQA metric CMDM achieves first place in PLCC and SRCC and the M4+M8 combination in the proposed method obtains the second rank in PLCC and SRCC. Since CMDM is full-reference and the proposed method is no-reference, it can be concluded that the proposed method is also effective at predicting the quality score of distorted meshes. Surprisingly, the FR 3D-to-2D metrics get remarkable performance results, among which MS-SSIM achieves the best performance. However, such methods highly rely on the quality of the projected 2D images, which can be easily affected by projected angles and viewpoints. But it proves the feasibility of FR 3D-to-2D metrics while NR 3D-to-2D metrics like BRISQUE and NIQE obtain mediocre performance.

Additionally, the P1+P2+P3+P4 combination represents feature groups with only color features and the P5+P6+P7+P8 combination represents feature groups with only geometry features. We can observe that, unlike the situations on the PCQA database, the color features and geometry features make nearly even contributions. Although many quantization distortions are introduced in the CMDM database, the groups including entropy values do not achieve the best performance. The Gamma distribution model (M4+M8) gets the highest performance in the proposed method, which represents that the Gamma distribution model is more effective on the CMDM database than other distribution models.

V. CONCLUSION

This paper proposes a no-reference colored 3D model quality assessment metric based on natural scene statistics. The proposed method deals with the quality assessment problems for both mesh and point cloud. We first project the 3D models into corresponding quality-related geometry and color feature domains. Then the statistic parameters are estimated using different distribution models to better capture the representative characteristics that are more in line with human perception. The proposed method is validated on the colored point cloud quality assessment database (SJTU-PCQA) and the colored mesh quality assessment database (CMDM), both of which include geometry distortions and color distortions. The experimental results show that our method outperforms the mainstream NR 3D-QA metric competitors and obtains an acceptable gap with the state-of-art FR 3D-QA metrics. The quality assessment we propose is quite standard and can be easily modified and expanded to satisfy specific needs, which has great application potential.

REFERENCES

- [1] H. Graf, S. P. Serna, and A. Stork, "Adaptive quality meshing for "on-the-fly" volumetric mesh manipulations within virtual environments," in *IEEE Symposium on Virtual Environments, Human-Computer Interfaces and Measurement Systems*, 2006, pp. 178–183.
- [2] "Apple developer document: Scanning and detecting 3d objects." [Online]. Available: https://developer.apple.com/documentation/arkit/content_anchors/scanning_and_detecting_3d_objects
- [3] "Intel realsense." [Online]. Available: <https://www.intelrealsense.com/>
- [4] Q. Yang, H. Chen, Z. Ma, Y. Xu, R. Tang, and J. Sun, "Predicting the perceptual quality of point cloud: A 3d-to-2d projection-based exploration," *IEEE Transactions on Multimedia*, pp. 1–1, 2020.
- [5] Y. Nehmé, F. Dupont, J. P. Farrugia, P. Le Callet, and G. Lavoué, "Visual quality of 3d meshes with diffuse colors in virtual reality: Subjective and objective evaluation," *IEEE Transactions on Visualization and Computer Graphics*, vol. 27, no. 3, pp. 2202–2219, 2021.
- [6] E. Alexiou, I. Viola, T. M. Borges, T. A. Fonseca, R. L. de Queiroz, and T. Ebrahimi, "A comprehensive study of the rate-distortion performance in mpeg point cloud compression," *APSIPA Transactions on Signal and Information Processing*, vol. 8, p. e27, 2019.
- [7] E. M. Torlig, E. Alexiou, T. A. Fonseca, R. L. de Queiroz, and T. Ebrahimi, "A novel methodology for quality assessment of voxelized point clouds," in *Applications of Digital Image Processing XLI*, vol. 10752. International Society for Optics and Photonics, 2018, pp. 174 – 190.
- [8] P. Cignoni, C. Rocchini, and R. Scopigno, "Metro: Measuring error on simplified surfaces," *Computer Graphics Forum*, vol. 17, no. 2, pp. 167–174, 1998.
- [9] R. Mekuria and P. Cesar, "Mp3dg-pcc, open source software framework for implementation and evaluation of point cloud compression," 2016, p. 1222–1226.
- [10] G. Lavoué, "A multiscale metric for 3d mesh visual quality assessment," *Computer Graphics Forum*, vol. 30, no. 5, pp. 1427–1437, 2011.
- [11] K. Wang, F. Torkhani, and A. Montanvert, "A fast roughness-based approach to the assessment of 3d mesh visual quality," *Computers and Graphics*, vol. 36, no. 7, pp. 808–818, 2012.
- [12] D. Tian and G. AlRegib, "BateX3: Bit allocation for progressive transmission of textured 3-d models," *IEEE Transactions on Circuits and Systems for Video Technology*, vol. 18, no. 1, pp. 23–35, 2008.
- [13] J. Guo, V. Vidal, I. Cheng, A. Basu, A. Baskurt, and G. Lavoué, "Subjective and objective visual quality assessment of textured 3d meshes," vol. 14, no. 2, 2016.
- [14] G. Meynet, Y. Nehmé, J. Digne, and G. Lavoué, "Pcqm: A full-reference quality metric for colored 3d point clouds," in *International Conference on Quality of Multimedia Experience*, 2020, pp. 1–6.
- [15] D. Tian, H. Ochimizu, C. Feng, R. Cohen, and A. Vetro, "Geometric distortion metrics for point cloud compression," in *IEEE International Conference on Image Processing*, 2017, pp. 3460–3464.

- [16] E. Alexiou and T. Ebrahimi, "Point cloud quality assessment metric based on angular similarity," in *IEEE International Conference on Multimedia and Expo*, 2018, pp. 1–6.
- [17] A. Javaheri, C. Brites, F. Pereira, and J. Ascenso, "A generalized hausdorff distance based quality metric for point cloud geometry," in *International Conference on Quality of Multimedia Experience*, 2020, pp. 1–6.
- [18] Z. Wang, A. Bovik, H. Sheikh, and E. Simoncelli, "Image quality assessment: from error visibility to structural similarity," *IEEE Transactions on Image Processing*, vol. 13, no. 4, pp. 600–612, 2004.
- [19] E. Alexiou and T. Ebrahimi, "Towards a point cloud structural similarity metric," in *IEEE International Conference on Multimedia Expo Workshops*, 2020, pp. 1–6.
- [20] Y. Liu, Q. Yang, Y. Xu, and L. Yang, "Point cloud quality assessment: Large-scale dataset construction and learning-based no-reference approach," 2020.
- [21] A. Mittal, A. K. Moorthy, and A. C. Bovik, "No-reference image quality assessment in the spatial domain," *IEEE Transactions on Image Processing*, vol. 21, no. 12, pp. 4695–4708, 2012.
- [22] Z. Wang, E. Simoncelli, and A. Bovik, "Multiscale structural similarity for image quality assessment," in *Asilomar Conference on Signals, Systems Computers*, vol. 2, 2003, pp. 1398–1402 Vol.2.
- [23] L. Zhang, L. Zhang, X. Mou, and D. Zhang, "Fsim: A feature similarity index for image quality assessment," *IEEE Transactions on Image Processing*, vol. 20, no. 8, pp. 2378–2386, 2011.
- [24] H. Sheikh and A. Bovik, "Image information and visual quality," *IEEE Transactions on Image Processing*, vol. 15, no. 2, pp. 430–444, 2006.
- [25] W. Sun, X. Min, G. Zhai, and S. Ma, "Blind quality assessment for in-the-wild images via hierarchical feature fusion and iterative mixed database training," 2021.
- [26] L. Váša and J. Rus, "Dihedral angle mesh error: a fast perception correlated distortion measure for fixed connectivity triangle meshes," *Computer Graphics Forum*, vol. 31, no. 5, pp. 1715–1724, 2012.
- [27] I. Abouelaziz, M. El Hassouni, and H. Cherifi, "No-reference 3d mesh quality assessment based on dihedral angles model and support vector regression," in *Image and Signal Processing*, 2016, pp. 369–377.
- [28] I. Abouelaziz, M. E. Hassouni, and H. Cherifi, "A convolutional neural network framework for blind mesh visual quality assessment," in *IEEE International Conference on Image Processing*, 2017, pp. 755–759.
- [29] I. Abouelaziz, A. Chetouani, M. El Hassouni, L. J. Latecki, and H. Cherifi, "No-reference mesh visual quality assessment via ensemble of convolutional neural networks and compact multi-linear pooling," *Pattern Recognition*, vol. 100, p. 107174, 2020.
- [30] S. Yang, C.-H. Lee, and C.-C. J. Kuo, "Optimized mesh and texture multiplexing for progressive textured model transmission," 2004, p. 676–683.
- [31] F. Caillaud, V. Vidal, F. Dupont, and G. Lavoué, "Progressive compression of arbitrary textured meshes," *Computer Graphics Forum*, vol. 35, no. 7, pp. 475–484, 2016.
- [32] E. M. Torlig, E. Alexiou, T. A. Fonseca, R. L. de Queiroz, and T. Ebrahimi, "A novel methodology for quality assessment of voxelized point clouds," in *Applications of Digital Image Processing XLI*, vol. 10752. International Society for Optics and Photonics, pp. 174 – 190.
- [33] A. K. Moorthy and A. C. Bovik, "Blind image quality assessment: From natural scene statistics to perceptual quality," *IEEE Transactions on Image Processing*, vol. 20, no. 12, pp. 3350–3364, 2011.
- [34] "Modified-brisque as no reference image quality assessment for structural mr images," *Magnetic Resonance Imaging*, vol. 43, pp. 74–87, 2017.
- [35] Q. Mérigot, M. Ovsjanikov, and L. J. Guibas, "Voronoi-based curvature and feature estimation from point clouds," *IEEE Transactions on Visualization and Computer Graphics*, vol. 17, no. 6, pp. 743–756, 2011.
- [36] T. Surazhsky, E. Magid, O. Soldea, G. Elber, and E. Rivlin, "A comparison of gaussian and mean curvatures estimation methods on triangular meshes," in *IEEE International Conference on Robotics and Automation*, vol. 1, 2003, pp. 1021–1026 vol.1.
- [37] P. Alliez, D. Cohen-Steiner, O. Devillers, B. Lévy, and M. Desbrun, "Anisotropic polygonal remeshing," 2003.
- [38] M. Corsini, E. D. Gelasca, T. Ebrahimi, and M. Barni, "Watermarked 3-d mesh quality assessment," *IEEE Transactions on Multimedia*, vol. 9, no. 2, pp. 247–256, 2007.
- [39] N. Mukherjee, "A hybrid, variational 3d smoother for orphaned shell meshes," in *IMR*, 2002.
- [40] H. Lee, P. Alliez, and M. Desbrun, "Angle-analyzer: A triangle-quad mesh codec," *Computer Graphics Forum*, vol. 21, no. 3, pp. 383–392.
- [41] I. Abouelaziz, M. El Hassouni, and H. Cherifi, "No-reference 3d mesh quality assessment based on dihedral angles model and support vector regression," in *Image and Signal Processing*, Cham, 2016, pp. 369–377.
- [42] Z. Wang and Q. Li, "Information content weighting for perceptual image quality assessment," *IEEE Transactions on Image Processing*, vol. 20, no. 5, pp. 1185–1198, 2011.
- [43] A. Mittal, R. Soundararajan, and A. C. Bovik, "Making a "completely blind" image quality analyzer," *IEEE Signal Processing Letters*, vol. 20, no. 3, pp. 209–212, 2013.
- [44] I. Abouelaziz, M. El Hassouni, and H. Cherifi, "A curvature based method for blind mesh visual quality assessment using a general regression neural network," in *International Conference on Signal-Image Technology and Internet-Based Systems*, 2016, pp. 793–797.